Citation for published version:

D. Codoni, et al., "Disc-shaped polyoxyethylene glycol glycerides gel nanoparticles as novel protein delivery vehicles", *International Journal of Pharmaceutics,* Vol. 496(2): 1015-1025, December 2015.

DOI:

https://doi.org/10.1016/j.ijpharm.2015.10.067

Document Version:

This is the Accepted Manuscript version.
The version in the University of Hertfordshire Research Archive may differ from the final published version. **Users should always cite the published version of record**.

Copyright and Reuse:

Enquiries

If you believe this document infringes copyright, please contact the Research & Scholarly Communications Team at rsc@herts.ac.uk

Disc-shaped polyoxyethylene glycol glycerides gel nanoparticles as novel protein delivery vehicles

Doroty Codoni[1,2], Jonathan Cowan[1], Jenna Bradley[1], William J. McAuley[3], Maria A O'Connell[1], Sheng Qi[1*]

Correspondence: Sheng Qi, sheng.qi@uea.ac.uk

[1] *School of Pharmacy, University of East Anglia, Norwich, Norfolk, UK, NR4 7TJ*
[2] *Procarta Biosystems Ltd, Innovation Centre, Norwich Research Park, Colney Lane, Norwich, UK, NR4 7GJ*
[3] *Department of Pharmacy, School of Life and Medical Sciences, University of Hertfordshire, Hatfield, UK, AL10 9AB*

Abstract:

Disc-shaped nanoparticles with high aspect ratios have been reported to show preferential cellular uptake *in vitro* by mammalian cells. However, engineering and producing such disc-shaped nanoparticles are often complex. This study reports for the first time the use of a single, approved pharmaceutical excipient to prepare stable disc-shaped nanoparticles with a high aspect ratio via a simple, organic solvent free process. These disc-shaped nanoparticles were formed by fragmentation of stearoyl macrogol-32 glycerides (Gelucire 50/13) hydrogels. The nanoparticles showed good physical stability as a result of their outer coating of polyethylene glycol (PEG) that is a part of Gelucire composition. Using lysozyme as a model hydrophilic protein, these nanoparticles demonstrated a good loading capacity for hydrophilic macromolecules, mainly via surface adsorption. As a result of the higher hydrophobicity of the core of the nano-discs, the loading efficiency of hydrophobic model components, such as Coumarin-6, was significantly increased in comparison to the model hydrophilic compound. These Gelucire nano-discs exhibited no cytotoxicity at the tested level of 600µg/ml for Caco-2 cells. Rapid *in vitro* cellular uptake of the disc-shaped nanoparticles by Caco-2 and H292 epithelial cells was observed. This rapid internalisation was attributed to the high aspect ratio of the disc-shape nanoparticles which provides a high contact surface area between the particles and cells and may lower the strain energy required for membrane deformation during uptake. The results of this study demonstrate the excellent potential of Gelucire nano-discs as effective nanocarriers for drug delivery and which can be manufactured using a simple solvent- free process.

Keywords: drug delivery, polyoxyethylene glycol glycerides, disc-shape nanoparticles, cellular uptake

Introduction

Nanoparticles have been studied intensively for targeted drug delivery and have received some success in diseases such as cancer (Wang et al., 2012). Anti-cancer efficacies of drug-loaded nanoparticles have been associated with the particle size and surface properties of the particles (Mitragotri, 2009). The conventional shape of the majority of nanoparticles studied and currently used in the clinic is spherical. In general, spherical nanoparticles with a diameter below 100 nm with surface modifications such as PEG or other surface ligand attachments show an enhanced permeation and retention effect (EPR), reduced surface plasma protein adsorption, prolonged *in vivo* circulation time and better tissue targeting (Alexis et al., 2008; Gref et al., 1994). However, recently an increasing number of studies have highlighted the importance of particle shape in the fate (such as circulation time, cellular uptake and biodistribution), cytotoxicity and potential efficacy of therapies that use nanoparticles (Truong et al. 2015; Agarwal et al., 2013; Barua et al., 2013; Sharma et al., 2010; Muro et al., 2008; Lu et al., 2013; Oh et al., 2010; Chu et al., 2014).

Among the different shapes of nanoparticles available, disc-shaped particles have shown some unique behaviour. For example, Agarwal and co-workers (2013) have reported the preferential cellular uptake of disc-shaped hydrogel nanoparticles by mammalian cells in comparison to spherical and rod-shaped hydrogel nanoparticles. The cytotoxicity of poly(3,4-ethylenedioxythiophene) nanoparticles with different shapes demonstrated increased cytotoxicity and apoptosis with decreasing the aspect ratios of the particles for the model cell lines studied (Hu et al., 2013). For drug delivery purposes, most reported disc-shaped nanoparticles have been made of PEG and polystyrene (Truong et al. 2015). These particles have shown high cellular uptake (Agarwal et al., 2013; Barua et al., 2013; Sharma et al., 2010; Muro et al., 2008). A full understanding of the mechanisms behind the enhanced *in vitro*

performance of disc-shaped nanoparticles is still lacking and there are limited reports of the types of materials and scalable preparation methods that can be used for the manufacture of disc-shaped nanoparticles (Truong et al., 2015). This study reports proof-of-concept results of the use of FDA approved, polyoxyethylene glycol glycerides, commercially known as Gelucire 50/13 to prepare disc-shaped gel nanoparticles using a scalable preparation method that does not require organic solvents or other additional processing aids.

Gelucire 50/13 is a mixed glycerides based material esterified with PEG. The rationale of choosing Gelucire 50/13 to prepare nanoparticles is based on both the constituent ingredients of this material and the bulk properties of Gelucire gels. The ability of glycerides based materials, such as the glycerylmonooleate (GMO), to form submicron particles (often with the aid of solvents) has been established (Gustafsson et al., 1996). However in order to obtain stable nanoparticle suspension formulations, the addition of stabilisers, such as surfactants, sugars, polymers (i.e. Poloxamer) and PEG, are often required (Spicer et al., 2001; Gustafssonet al., 1997). Gelucire intrinsically contains free PEG and has been used as a stabiliser of solid lipid nanoparticles (SLN) and nanostructured lipid carriers (NLC) (Date et al., 2011). The presence of PEG in Gelucire may also provide the surface modification required to increase the half-life of nanoparticles in the bloodstream by reducing the metabolic degradation and the immunogenicity of the nanoparticle (Almeida and Souto, 2007). Therefore in theory, the 8% free PEG 1500 and the small proportions of monoacyl and diacyl PEG in Gelucire 50/13 may act as an intrinsic stabiliser if used for the production of nanoparticles, suggesting that Gelucire 50/13 gels would be good candidates for producing gel nanoparticles. However, to date, there is no published work that has explored the ability of using Gelucire 50/13 alone to form stable nanoparticles.

The unique bulk properties of Gelucire 50/13 based gels include their semi-liquid crystalline structures, which evolve from lamellar to hexagonal and cubic phases depending on the water content of the gels (Qi et al., 2010; Codoni et al., 2015). For the gels with intermediate to high water contents structural analyses suggest the possibility of the co-existence of multiple liquid crystalline phases. Our previous rheological studies have shown the formation of cross-linked or entangled structures depending on the water content of the gels (Codoni et al., 2015). Detailed analysis of the microstructures of the gels using SEM, DSC and relaxometry NMR confirmed the existence of water compartments (such as aqueous channels and domains) in the interior of the gels (Codoni et al., 2015). This ordered network structure of the gels offers the potential of forming nanoparticles by mechanical fragmentation.

The aim of this study was to develop a robust method for preparing nanoparticles based on Gelucire 50/13 gels alone. Lysozyme was employed as a model hydrophilic protein and the characterisation of the lysozyme-loaded nanoparticles as well as the encapsulation efficiency and the retained activity of lysozyme were assessed. Coumarin-6 was used as a highly hydrophobic model component for comparing the loading efficiency of materials with different hydrophobicities. *In vitro* cytotoxicity of the nanoparticles was assessed using two human epithelial cell model lines, the lung cancer cell line (H292) and the human intestinal cell line (Caco-2). The cellular uptake of the gel nanoparticles was also evaluated using Caco-2 cells.

Experimental

Materials

Stearoyl macrogolglycerides (Gelucire® 50/13) was kindly donated by Gattefossé SAS (St Priest, France). Hen egg-white lysozyme (Sigma Aldrich, Gillingham, UK) was used the chosen model protein. Ultrapure type I water (Milli-Q grade, 18 MΩ.cm at 25 °C) produced by

Barnstead Nanopure system (Thermo Scientific, UK) was used for all the sample preparations. Coumarin 6 (3-(2'-Benzothiazolyl)-7-diethylaminocoumarin) was used as lipophilic fluorescent dye (Acros Organics, USA). *Micrococcus lysodeikticus* cells were purchased from Sigma Aldrich, UK. Foetal calf serum (FCS) was purchased from Biosera, UK. DMEM (Dulbecco's Modified Eagles Medium with glucose and glutamine), 10,000 U/ml penicillin and 10,000 μg/ml streptomycin, 0.25% trypsin-EDTA were purchased from Invitrogen, UK. Non-essential amino acids and sodium pyruvate were purchased from Thermo Fisher Scientific,UK. For the MTS assay the CellTilter96® AQ$_{ueous}$ One Solution (Promega) was used.

Preparation of protein loaded gel nanoparticles

The gel nanoparticles were prepared by fragmentation of Gelucire 50/13 bulk gel in water. A range of Gelucire 50/13 gels with water contents from 10% to 90% (w/w) were prepared by melting Gelucire at 62 ± 2 °C. The appropriate amount of water, heated to the same temperature, was added to the melted Gelucire. The mixtures were removed from the heat and a hand-held disperser (Power Gen 125, Fischer Scientific, UK) was used for agitating the mixture at 8000 rpm for 2-3 minutes. After adding water to the bulk gel with a weight ratio of 9:1 gel: water, bulk gel fragmentation was performed by vortexing the gel using a hand-held disperser (Ultra Turrax T10 basic, IKA, Germany) at 30000 rpm for 5 minutes. The nanoparticle dispersion with a final concentration of 2% w/w gel and 98% w/w water was homogenised by passing it five times through a high-pressure homogeniser (EmulsiFlex-C5, Avestin, Ottawa, Canada) at the pressure of approximately 12000 psi and at room temperature. The nanoparticles made from the bulk gels with 40, 50, and 60% water contents were labelled as F1 to F3, respectively (as seen in Table 1). The formulations were stored at 4 °C and at room temperature for the physical stability studies.

Preparation of the lysozyme-loaded gel nanoparticles followed the same procedure for fragmenting lysozyme-loaded bulk gels. Lysozyme was incorporated into the gels with 40% to 60% (w/w) water contents by pre-dissolving lysozyme in the water phase. The lysozyme concentrations in the gel formulations were fixed at 3% (w/w) for all formulations. The final concentration of lysozyme in the nanoparticle dispersion is 0.06 mg/ml. The components of the formulations are listed in Table 1.

Table 1. Water content of the bulk gels and their corresponding gel nanoparticles

Protein-free bulk gel formulations (water, w/w)	Gel nanoparticle formulations	Lysozyme-loaded bulk gel formulations (% water, w/w)	Gel nanoparticle formulations
40	F1	40	F1-LYS
50	F2	50	F2-LYS
60	F3	60	F3-LYS

Dynamic Light Scattering (DLS)

The size of the nanoparticles in aqueous suspension was analysed with a DLS (Zetasizer Nano, Malvern Instruments Ltd, Malvern, UK) in backscattering mode (173°). The samples were equilibrated at 37 ° C for 15 minutes and three acquisitions were taken for each sample. The samples were analysed in triplicate. The physical stability tests of the nanoparticles suspension formulations were performed on the formulations stored at room temperature and at 4 °C over a period of time for 4 months. The size distribution obtained is derived from the intensity calculation (NNLS) performed by the Zetasizer software, 6.20. All measures were repeated 4-6 times.

Atomic force microscopy (AFM)

The sizes and shapes of the selected lysozyme-free and lysozyme-loaded nanoparticle formulations (F1 and F3) were analysed using a Caliber atomic force microscope (AFM) from

Bruker AFM (UK). The formulations were diluted 1:10 with Milli-Q water and 3 µl of the dilution were dropped on a mica film and left to dry for 15 minutes. The film was then rinsed with water and dried with compressed air. As the nanoparticles show little tendency for aggregation (see stability results), it was assumed that the dilution and drying process applied would not lead to significant changes in the sizes of the nanoparticles. Five to ten sites on each sample were analysed in order to assess the level of homogeneity of the formulations.

Cryo-Transmission electron microscopy (Cryo-TEM)

Cryo-TEM was used to assess the size and shape of the gel nanoparticle formulations F1 and F3. The nanoparticles were placed on the microscope copper grid (coated with a perforated polymer film) in order to form a thin aqueous film. The excess of liquid was removed by blotting with a filter paper. The film was then immersed in a cooling medium (ethane) held at a temperature just above its freezing point. The film rapidly vitrified without crystallisation. The grid with the vitrified film was transferred to a Zeiss EM 902 A transmission electron microscope (Oberkochen, Germany). The sample was held at liquid nitrogen temperature and at a controlled humidity environment during the measurement. All observations were made in zero-loss bright-field mode and at an accelerating voltage of 80 kV. The nanoparticles suspensions were analysed non-diluted and at a maximum magnification of 50000x.

Encapsulation efficiency (%EE)

The centrifugation method was chosen to assess the encapsulation efficiency of lysozyme in the nanoparticle formulations. A 3 ml sample of the nanoparticle aqueous suspension was loaded in the centrifugal filter tubes (Amicon Ultra-4, Millipore) with regenerated cellulose membrane (MWCO 30 kDa) and centrifuged at 2000 g (Heraeus, Thermo Scientific, UK) for a period of time that allowed the collection of 2.5 ml of filtrate solution. The filtrate solution

collected after centrifugation was analysed with a UV spectrometer to assess the quantity of lysozyme. The quantification of the encapsulation efficiency was calculated using the following formula

$$EE\% = \frac{F\,lys_t - F\,lys_c}{F\,lys_t} \qquad \text{Eq. 1}$$

where $F\,lys_t$ is the total amount of lysozyme loaded in the formulation and $F\,lys_c$ is the amount of free lysozyme recovered in the filtrate after centrifugation.

Prior to the analysis, a calibration curve of lysozyme in aqueous solution was constructed. A lysozyme aqueous solution with a concentration of 0.9 mg/ml (0.09 % w/v) was prepared as the stock solution. 1, 2, 3, 4 and 5ml aliquots of the stock solution were then individually transferred in 10 ml volumetric flasks to prepare dilutions of lysozyme solutions with concentrations of 0.09, 0.18, 0.27, 0.36 and 0.45 mg/ml, respectively. Three repetitions were used and the average UV absorbance values of the solutions were plotted against the protein concentrations. The measurements were taken using a UV spectrophotometer (Lambda 35, Perkin-Elmer, USA). The wavelength of maximum absorbance, λmax, 280 nm was used for the measurements. All encapsulation measurements for each formulation were performed at least in triplicate.

Lysozyme activity assay

The biological activities of lysozyme in solution and formulations were tested by measuring the degree of lysis induced by lysozyme on *micrococcus lysodeikticus* cells using a turbidimetry test described by Shugar (1952). The test is based on the comparison of the decrease in turbidity of the suspension and therefore the decrease of absorbance at 450 nm of a lysozyme solution with the known activity. A 0.015% (w/v) *micrococcus lysodeikticus* cell

suspension was prepared using 66 mM potassium phosphate buffer (pH=6.27) at 25 °C. Immediately before the test, a lysozyme buffer solution was prepared to contain 400 U/ml of the protein as control. The lysozyme-loaded nanoparticle formulations with a lysozyme concentration equal to 0.6 mg/ml were diluted with the phosphate buffer to obtain a final concentration of lysozyme equal to 0.01 mg/ml.

The tests were performed by pipetting 2.5 ml of the substrate (*micrococcus lysodeikticus*) into a quartz cuvette and leaving it to equilibrate at 25 °C for five minutes. A 100 µl sample of the phosphate buffer (for the blank control) or the diluted nanoparticle formulation was then added and mixed by inversion. The absorbance of the tested solution at 450 nm was measured every 10 seconds over a period of 5 minutes. The decreases in absorbance were plotted against the time. The biological activity of lysozyme expressed in units/ml was calculated according to the protocol described by Shugar (1952).

Circular Dichroism (CD)

CD spectroscopy was used to study the changes in the lysozyme conformation after incorporation into the gel nanoparticle formulations. CD spectra were acquired in the near UV (240-500 nm) for lysozyme aqueous solution (0.6 % w/w) and for lysozyme-loaded nanoparticles dispersions with lysozyme concentration of 0.6 mg/ml (w/w). The concentration of the lysozyme in the nanoparticles suspension and in the aqueous solution was fixed at 0.6 mg/ml. The tests were performed in triplicate by using a JASCO J-810 spectropolarimeter (Tokyo, Japan). A quartz cuvette with 10 mm pathlength was used.

In vitro cytotoxicity and cellular uptake studies

In vitro cytotoxicity of the unloaded nanoparticle formulation F2 was tested by using a model human lung epithelial cell line, H292 and human colon epithelial cell line, Caco-2 (from

ECACC). Both cell types were cultured in RPMI 1640 media containing 10% foetal calf serum, 100 U/ml penicillin, 100µg/ml streptomycin and 2mM L-glutamine. Cells were maintained between 0.3-1 x10^6/ml at 37ºC and 5% CO_2 and detached from culture flasks with 0.25% trypsin-EDTA. The nanoparticles were prepared from the bulk gel with 40% water and the dispersion had a final lipid concentration of 12 mg/ml. Caco-2 and H-292 cells were plated at 4 x 10^3/100 µl in 96 well plates and a range of dilutions of the formulation F2 (600, 300, 200, 150, 120, and 100 µg/ml) were added to the cells for 24 or 48h. Cell viability was measured by MTS assay as previously described (Howell et al, 2012) or by trypan blue exclusion using 0.4% trypan blue (Sigma).

The fluorescently labelled Gelucire 50/13 gel nanoparticles used for the cellular uptake study were prepared using the heating method. The fluorescent dye (Coumarin-6) was added to the melted lipid and mixed using a magnetic stirrer. When the dye was completely dissolved in the molten lipid, water heated to the same temperature as the molten lipid was added and the nanoparticles were prepared following the same steps described earlier. The concentration of Coumarin-6 in the gels is 0.001% w/w. The fluorescently labelled gel nanoparticles were prepared by following the same procedure described above. Caco-2 cells were plated at 1 x 10^5 cells/ml in 6 well plates and adhered overnight. The gel nanoparticles were added for various times up to 24 h and examined by microscopy using a Leica MS GmbH fluorescence microscope and Leica Application Suite software (Leica, Mannhein, Germany).

Results and discussion

Fabrication of disc-shaped gel nanoparticles

The simple three-step aqueous fabrication process of the disc-shaped Gelucire nanoparticles is shown in Figure 1. A room temperature lysozyme solution was added into pre-melted Gelucire. With vigorous agitation of the mixture at room temperature, it gradually set into a bulk gel.

Additional amount of water was added to the bulk gel with the ratio of 9:1 (w/w) and electrical disperser was used to break down the bulk gel to coarse particles. Gelucire gel nanoparticles were then obtained via high-pressure homogenisation of the coarse particles. Two key variables for the nanoparticle formulations are the total water content in the bulk gel and the lysozyme loading. It can be seen in Figure 2 that the total water content of the bulk gel has a clear impact on the processability and particle size of nanoparticles. Gels with higher water content have a smaller mean particle size, but all formulations have two populations of sizes with polydispersity PDI value ≥ 0.3. More importantly, a higher water content of the bulk gel also leads to the production of nanoparticles with sizes that are independent of repeated processing by high-pressure homogenisation. This is likely to be a result of different self-assembled microstructures of the bulk gels with different water contents. As discussed in our previous work, the SAXS results of gels with intermediate water content (40-60%) indicated the presence of cubic and hexagonal configurations, whereas the gels with low water contents tend to predominantly consist of a lamellar structure (Qi et al., 2010). The 3D assembled structure of the gels with cubic and hexagonal molecular arrangements have a greater degree of freedom and higher degree of chaoticity within the structure which may facilitate their natural breakdown into nanoparticles, whereas lamellar gels have a much denser 2D structure and as such the particle size of the fragmented lamellar based bulk gel may be progressively reduced by repeated high-pressure homogenisation.
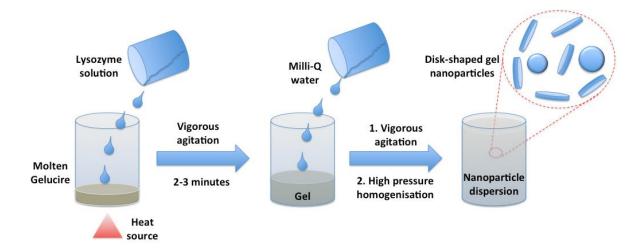
Figure 1. Schematic illustration of the fabrication process of lysozyme-loaded disc-shaped gel nanoparticles

DLS was used in the first instance to measure the hydrodynamic particle size of the gel nanoparticles. For lysozyme-free nanoparticles, F1 showed significant reduction in particle size with increasing the homogenisation cycles from 1 to 3. After 5 cycles of homogenisation, the particle size remained constant at approximately 120 nm with a small population of particles at 20 nm (Figure 2). A clear bimodal distribution was observed for the F2 and F3 formulations with the main population being between 120-200 nm, and the second population being about 20 nm. The presence of lysozyme increased the polydispersity and the sizes of the main population of the nanoparticles in comparison to the corresponding unloaded nanoparticles (Figure 3).
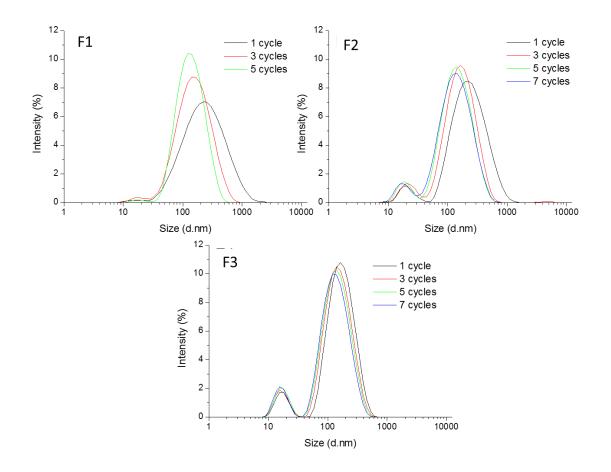
Figure 2. Changes of size distribution (d.nm) of the nanoparticle formulations F1, F2 and F3 prepared by being passed through the high-pressure homogeniser with different number of cycles (n≥3).
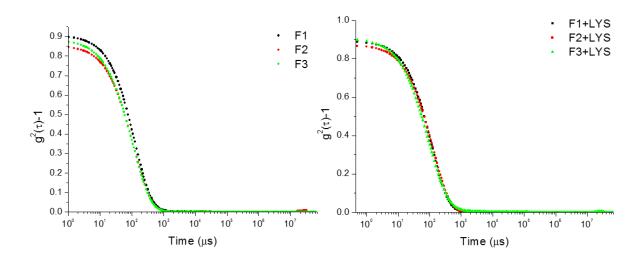

Figure 3. DLS correlation functions of the nanoparticle formulations (a) without and (b) loaded lysozyme measured at 37 °C.

Although the DLS can provide estimation of the hydrodynamic diameter of the nanoparticles, the analysis is based on the assumption of the particles being spherical. Therefore, in order to obtain more detailed information of the shape of the nanoparticles, cryo-TEM and AFM analyses were carried out. An example cryo-TEM image of F3 formulations is shown in Figure 4. It is clear that the Gelucire nanoparticles have low-contrast to the surrounding media due to the presence of PEG chain which is invisible to the electron beam. This has been documented previously in the literature (Zetterberg et al., 2011), nevertheless the disc-like shape of the nanoparticles with the disc-face ranging between 50 and 300 nm and the disc-edge thickness ranging from 7-10 nm can be identified in the images. The low thickness of the discs in comparison to the dimensions of the disc-face of the nanoparticles gives the high aspect ratio (the ratio between the longer and short dimensions of the 2D object) of these nano-discs. More than 100 nanoparticles from each formulation were analysed and the diameter of the disc-face of the nanoparticles was determined using ImageJ 1.46r software. Histograms of the frequency (number of particles within a certain size range) versus the particle size were plotted using OriginPro 8. It can be seen that a high proportion of particles have a disc-face diameter between 150-300 nm. This is in good agreement with the DLS results.
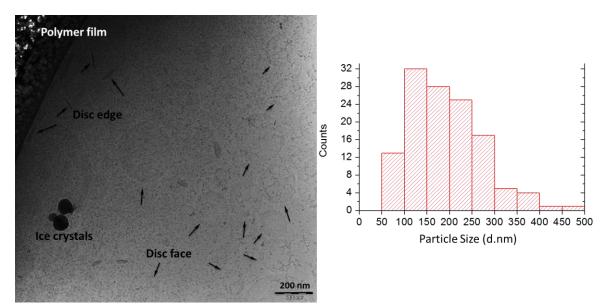

Figure 4. (a) Example cryo-TEM image and (b) histogram of the particle size distribution of

the F1 formulation, measured from cryo-TEM images (plotted using frequency versus size interval).

The 3D shape information of the nanoparticles was further studied using AFM. Tapping mode was used for all measurements, in order to minimise the damage of the soft Gelucire nanoparticles. As seen in Figure 5, using topographic analysis, the thickness and diameter of individual disc-shaped particles can be revealed. The data is summarised in Table 2, where all nanoparticles show high aspect ratios (X/Y:Z) of between 28:1 to 9:1, with F1 nanoparticles having the highest aspect ratio. The disc-face of F1 and F2 are largely circular in shape, whereas that of F3 shows a more elliptical shape. Lysozyme loading led to an increase in all of the dimensions of the particles. The sizes measured by DLS and cryo-TEM are slightly bigger than the ones obtained by AFM. This is likely to be due to the drying step of the samples preparation of AFM measures led to the loss of hydrodynamic radius of the nanoparticles. Both cryo-TEM and AFM confirmed the disc-shape of the Gelucire nanoparticles. The high aspect ratio in combination with the disc shape may contribute to the cellular uptake behaviour of the nanoparticles which is discussed later.
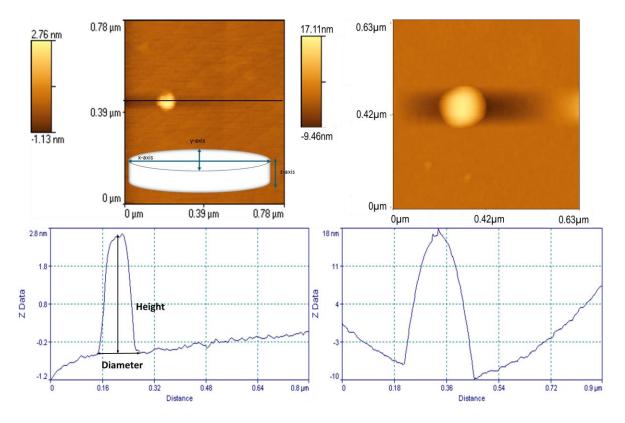
Figure 5. Tapping mode AFM images of an example of the unloaded F1 (left) and lysozyme loaded (right) nanoparticle formulation F1-LYS.

Table 2. Dimensions (as illustrated in Figure 4) of the Gelucire nanoparticles in different formulations determined using AFM (n=8-10±SE)

Formulation	Unloaded native nanoparticles		
	X axis (Disc-face diameter 1)	*Y axis (Disc-face diameter 2)*	*Z axis (Thickness)*
F1	84±4.93	62±9.29	3±0.6
F2	96±7.92	110±13.99	9±1.8
F3	77±1.41	78.5±4.95	9±0.6
Formulation	LYS loaded nanoparticles		
	X axis (Disc-face diameter 1)	*Y axis (Disc-face diameter 2)*	*Z axis (Thickness)*
F1-LYS	207±5.60	184±6.91	27±0.9
F3-LYS	142±4.37	139±8.56	12±1.2

Protein-loading efficiency and physical stability of disc-shaped gel nanoparticles

The lysozyme loading efficiency of the nanoparticles showed formulation dependency, but particle size independency. For the F1-LYS nanoparticle formulations, the lysozyme was encapsulated with higher efficiency (38%) than for the F2-LYS and F3-LYS formulations (33% and 29%, respectively). Overall, the encapsulation efficiency of lysozyme in the nanoparticle formulations decreases with increasing water content in the bulk gel used to prepare the nanoparticles. This may indicate that the encapsulation efficiency may be related to the different microstructures of the bulk gels (Codoni et al., 2015).

The physical stabilities of the gel nanoparticle formulations were studied by monitoring the particle size of the nanoparticles using DLS. The mean size diameters of all lysozyme-free nanoparticles stored at room temperature over a period of two weeks showed no significant change (Table 3). At 4°C over a 4-month storage period, no particle size changes were observed for any of the formulations indicating that no aggregation or degradation of the particles occurred over these time frames. For the formulations loaded with lysozyme, despite little change being observed in particle size, a precipitate was observed after 14 days of aging at room temperature for the F1-LYS nanoparticles (Table 4). This is likely to be associated with the lysozyme instability at room temperature in solution. However, the lysozyme-loaded nanoparticles stored at 4 °C were stable over the period of 4 months with no precipitation or significant particle size change.

Table 3. Hydrodynamic size distribution (d.nm) of the unloaded nanoparticles stored at different temperatures and monitored overtime using DLS (n=3; NA= Not Analysed)

Formulations stored at 4°C	Population 1				Population 2			
	Time (days)				Time (days)			
	7	14	30	120	7	14	30	120

Formulations								
F1	—	—	—	—	163±3.15	157±2.35	153±0.94	179±35.37
F2	20±0.19	18±0.52	NA	19±0.68	160±1.54	159±3.18	NA	163±9.41
F3	17±0.43	17±0.35	NA	16±2.75	153±4.12	156±2.74	NA	152±5.81
Formulations Stored at 20°C	*Time (days)*				*Time (days)*			
	1	*2*	*7*	*14*	*1*	*2*	*7*	*14*
F1	—	—	—	—	151±4.88	154±3.92	160±5.45	162±2.82
F2	21±0.89	19±1.47	19±0.39	19±0.60	163±2.50	161±1.14	161±0.37	161±0.88
F3	17±0.47	17±0.61	17±0.35	17±0.60	158±1.79	160±0.06	157±0.27	156±0.41

Table 4. Hydrodynamic size distribution (d.nm) of the lysozyme loaded gel nanoparticles stored at different temperatures and monitored overtime using DLS (n=3; NA= Not Analysed)

Formulations stored at 4°C	*Population 1*				*Population 2*			
	Time (days)				*Time (days)*			
	7	*14*	*30*	*120*	*7*	*14*	*30*	*120*
F1-LYS	—	—	—	—	147±4.28	151±1.86	148±0.91	151±1.11
F2-LYS	18±0.27	18±2.09	19±1.03	NA	174±7.1	178±3.97	177±1.08	NA
F3-LYS	17±0.55	17±0.68	17±0.26	NA	139±4.04	136±4.04	139±0.05	NA
Formulations Stored at 20°C	*Time (days)*				*Time (days)*			
	1	*2*	*7*	*14*	*1*	*2*	*7*	*14*
F1-LYS	—	—	—	—	155±9.18	150±2.57	NA	NA
F2-LYS	18±0.27	18±2.09	19±1.03	—	183±0.74	NA	NA	179±3.70
F3-LYS	17±0.27	18±0.48	18±0.36	17±0.34	139±4.74	138±2.46	143±2.78	146±5.51

Incorporation of lysozyme into the gel nanoparticles may affect its biological activity. Therefore the retained biological activities (RBA%) of lysozyme in different gel nanoparticles were measured using the micrococcus lysodeikticus assay. As shown in Table 5, the native lysozyme solution retains 46% activity at room temperature immediately after preparation. After incorporation into the gel nanoparticles, the activity increased to 59% for F1-LYS, but reduced to ~20% for F2-LYS and F3-LYS (which were prepared from the gels with higher water content). It is noted that F1-LYS also has the highest lysozyme encapsulation efficiency. The higher retained activity in the formulation F1-LYS may indicate that the formulation protects the lysozyme from degradation and helps to retain its activity.

Table 5. Lysozyme loading capacity and retained biological activity (% RBA) in the Gelucire gel nanoparticles

Formulations	Loading capacity (%)	% RBA
F1-LYS	38	59
F2-LYS	33	21
F3-LYS	29	19

Near UV circular dichroism was further used to investigate any tertiary structural changes of lysozyme following its incorporation into the gel nanoparticles. In the near UV region, the spectrum arises from the aromatic amino acids of the proteins, such as Tryptophan (Trp), Tyrosine (Tyr), Phenylalanine (Phe) and disulfide bridges. In general, Trp shows a peak in the region between 290 and 305 nm, the Tyr between 275 and 282 nm and the Phe between 255 and 270 nm (Kelly et al., 2005). In a lysozyme molecule, the Trp is the most present aromatic amino acid with 6 residues per molecule, while the Tyr and Phe have 3 residues each (Jollès, 1969). CD spectra (Figure 6) were obtained from the aqueous suspensions of F1-LYS, F2-LYS and F3-LYS nanoparticles. Aqueous lysozyme solution and unloaded nanoparticles suspensions were also analysed as controls. The peaks at 290 nm, associated with the Trp residues, are visible in the spectra of all formulations. From the CD spectra it is clear that lysozyme retains its tertiary structure in the nanoparticles F2-LYS and F3-LYS, which were prepared from the gels with higher water contents, while subtle differences in peaks associated the Phe are noted for formulations F1-LYS. In formulations F1-LYS the peak at 284 nm is less intense, but the peak at 281 nm is more evident. However, despite the slight alternation of the tertiary structure of the lysozyme, F1-LYS nanoparticles still ensures the retaining of the biological activity of lysozyme in the formulations, which indicates the alternation is insignificant to the biological activity of lysozyme.
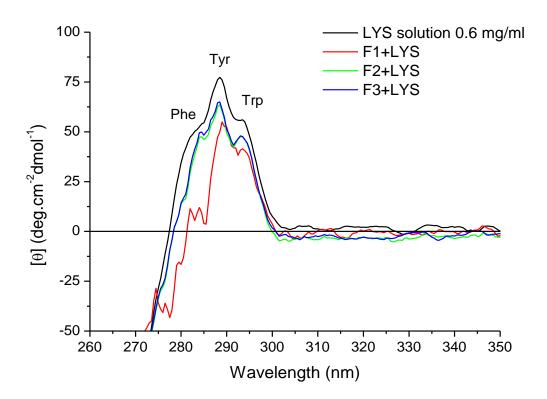
Figure 6. Near UV CD spectra of lysozyme solution and lysozyme-loaded nanoparticles

Building molecular model of Gelucire nanoparticles

Using the physicochemical characterisation obtained above in combination with the molecular properties of Gelucire reported in literature (Brubach et al., 2004), the structure of the protein loaded Gelucire nanoparticles is proposed in Figure 7. Because the nanoparticles are in aqueous solution, the polar head of the glycerides and the PEG chains are likely to be located on the surface of the particles, while the hydrophobic fatty acid chains (C_{16} and C_{18}) are enclosed in the inner compartment of the nanoparticles. The presence of the free low molecular PEG (MW 1500) on the surface of the nanoparticles could also explain the good physical stability of the formulations (Date et al., 2011). The nanoparticles were confirmed to have a disc-like shape by cryo-TEM and AFM. The thickness of the nanoparticles agrees well with the length of the glycerides aliphatic chains (4.5-5 nm) indicating the interpenetration nature of glycerides in these nano-discs (Brubach et al., 2004). This also implies that these nano-discs are not likely

to have a hydrophilic centre as with the classic bilayer, liposome type of colloid, but are more likely to have a hydrophobic core which could act as effective encapsulation/solubilisation compartments for poorly soluble compounds. This was confirmed by the 100% encapsulation efficiency of Coumarin-6, a hydrophobic compound that can also be used as fluorescent dye, in the Gelucire nanoparticles.
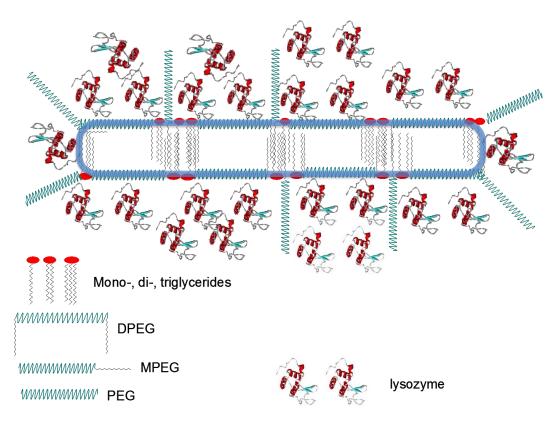

Figure 7. Schematic illustration of nanostructure of the disc-shaped Gelcuire 50/13 gel nanoparticles loaded with model protein drug.

As the nanoparticles are disc-like shape with restricted dimensions, hydrophilic macromolecules such as lysozyme cannot be fully loaded within the hydrophobic interior of the nanoparticles. Instead, it is more likely that lysozyme may interact with the polar part of the surface of the nanoparticles. This interaction may anchor the lysozyme molecules at the surface of the nanoparticles. As a result, the loading of lysozyme increases the size of the nanoparticles. However, a relatively low encapsulation efficiency would be expected in this

scenario as only the nanoparticle surfaces are used to load the protein, thus per particle only limited number of lysozyme molecules can be loaded. This also explains the reduced physical stability of lysozyme-loaded nanoparticles. The surface adsorbed proteins are likely to increase aggregation between particles.

In vitro cytotoxicity and cellular uptake of disc-shaped gel nanoparticles

As the F1 nanoparticle formulation has many promising properties such as good physical stability and encapsulation efficiency and a high level of retained activity of the encapsulated lysozyme, its potential as carrier for protein delivery was further explored. The *in vitro* cytotoxicity of the unloaded nanoparticle formulation F1 was tested using a model human lung epithelial cell line, H292 and a human colon epithelial cell line, Caco-2. As seen in Figure 7a, the F1 formulation with a concentration of 600 µg/ml of total Gelucire was toxic to H292 cells, reducing cell viability in the MTS assay by 71%. The results of the other dilutions (up to 300 µg/ml) of the placebo F1 nanoparticles showed satisfactory cell viability by MTS assay (Figures 8a). The effect of the F1 nanoparticle suspension on Caco-2 cell viability was also assessed by the MTS assay. As seen in Figure 8b, Caco-2 cells show better tolerance to Gelucire nanoparticles than H292 cells. No cytotoxicity was observed even at a 600 µg/ml concentration.
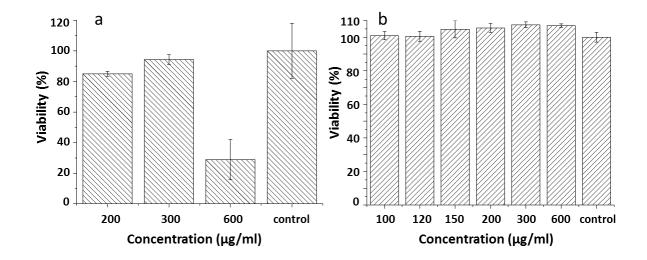
Figure 8. *In vitro* cell viability of (a) H292 cells and (b) Caco-2 cells incubated with F1 nanoparticle suspensions with different nanoparticle concentrations at 37°C for 24 hours as determined by the MTS assay. Viability is calculated as a percentage of the control (n=3).

The *in vitro* cell uptake of formulation F1 was investigated using Caco-2 cells. In order to be able to assess uptake, fluorescently labelled nanoparticles containing Coumarin-6 were prepared. The labelled F1 nanoparticle dilutions with final concentrations of total Gelucire of 300 and 120 µg/ml were used to incubate Caco-2 cell monolayers. As seen in Figure 8a and b, after 15 minutes of incubation, it is evident that the cellular internalisation is significant. No significant differences were observed after 120 minutes of incubation indicating the uptake is rapid and complete within the first 15 minutes of exposure to the nanoparticles. The non-toxic and rapid internalisation features of the nanoparticles are further demonstrated by non-changed results of F1 nanoparticles after 4 and 24 hours incubation periods in Figure 9.
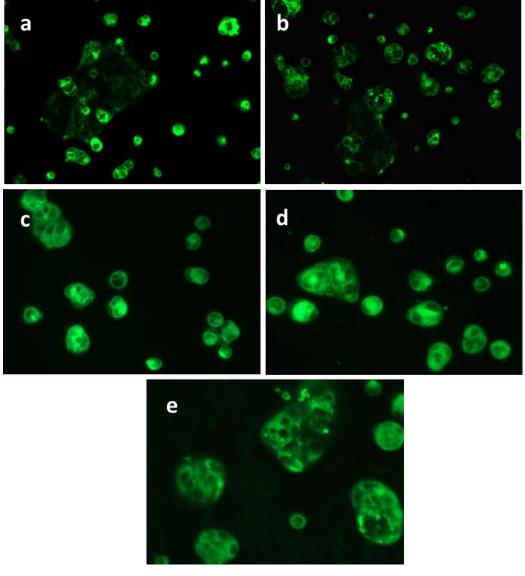
Figure 9. Fluorescent light microscopic images of *in vitro* Caco-2 cellular uptake of the F1 nanoparticles from dilutions (a) D1 and (b) D4 after 15 minutes of incubation; and (c) D2 after 30 minutes of incubation (d) D2 after 4 hours of incubation and (e) D2 after 24 hours incubation. Images of a-b, c-d, and e were taken using objectives with 10X, 40X, and 63X magnification, respectively.

Although the mechanism by which the nanoparticles were taken up by the Caco-2 cells remains unclear and further studies will be required, it is most likely that Coumarin-6 uptake occurred when loaded within the nanoparticles. Li and co-workers (2011) reported similar results on the cellular uptake of Coumarin 6-loaded liposomes modified by Pluronic. The study suggests that

due to high hydrophobicity, the amount of Coumarin 6 detected within the cells should be taken up through the interaction between the cells and liposomes. Therefore, the possibility that Coumarin 6 diffused within the cells after being released from the liposomes was excluded. A similar mechanism would also be expected to apply in this case. More importantly, the disc-shape and high aspect ratio of the Gelucire nanoparticles is expected to also contribute to the rapid internalisation of the nanoparticles. As reported by Agarwal and co-workers (2013), the disc-shaped hydrophilic nanoparticles with high aspect ratios have preferable internalisation in vitro conditions for mammalian epithelial and immune cells. This rapid internalisation in vitro has been attributed to a complex interplay of three shape- and size-dependent parameters including particle surface area available for cell contact, strain energy for membrane deformation, and local particle concentration at the cell membrane (Agarwal et al., 2013).

Conclusions

This study has demonstrated the ability of Gelucire 50/13 gels to be mechanically fragmented into stable disc-shaped nanoparticles. The unique preparation method of the disc-shape nanoparticles reported in this study is relatively inexpensive, organic solvent free and does not require the addition of any stabilisers. The nanoparticles are with DLS measured mean size between 20-300nm and polydispersity of the disc-shape nanoparticles showed formulation (water content in the bulk gel) dependency. All characterisation techniques used including cryo-TEM, DLS and AFM showed good agreement on the size and shape analysis of the nano-discs. All formulations (with and without lysozyme) showed good physical stability at 4°C, however lysozyme loading led to an increased tendency for aggregation on storage at room temperature. Lysozyme was used as model protein loaded to the nanoparticles. A good efficiency of loading of the lysozyme was achieved with nearly 60% retained biological activity of lysozyme in the formulations with higher Gelucire content. These formulations showed increased particle size

with a larger disc surface which may contribute to accommodate a larger amount of lysozyme in comparison to the nano-discs with smaller surface areas. The nanoparticles were shown to be non-toxic to the H292 cells up to 300 μg/ml Gelucire concentration, and at least 600 μg/ml for the Caco-2 cells. The cellular uptake of the nanoparticles by Caco-2 cells is rapid and stable up to 24 hours. The rapid cellular uptake was attributed to the disc-shape and high aspect ratio of the gel nanoparticles. The outcome of this study provides prove-of-concept evidence of the potential use of this ready-to-use nano-disc formulation for macromolecule delivery.

Acknowledgment and Disclosures:

References

Agarwal, R., Singh, V., Jurney, P., Shi, P.L. Sreenivasan, S.V., Roy, K., 2013. Mammalian cells preferentially internalize hydrogel nanodiscs over nanorods and use shape-specific uptake mechanisms. Proceedings of the National Academy of Sciences 110, 17247-17252.

Alexis, F., Pridgen, E., Molnar, L.K., Farokhzad, O.C., 2008. Factors Affecting the Clearance and Biodistribution of Polymeric Nanoparticles. Molecular Pharmaceutics 5, 505-515.

Almeida A.N.J., Souto, E., 2007. Solid lipid nanoparticles as a drug delivery system for peptides and proteins. Advanced Drug Delivery Review 59, 478-490.

Barua, S., Yoo, J.W., Kolhar, P., Wakankarc, A., Gokarnc, Y.R., Mitragotria, S., 2013. Particle shape enhances specificity of antibody-displaying nanoparticles. Proceedings of the National Academy of Sciences 110, 3270-3275.

Brubach, J.B., Ollivon, M., Jannin, V., Mahler, B., Bourgaux, C., Lesieur, P., Roy, P., 2004.

Structural and Thermal Characterization of Mono- and Diacyl Polyoxyethylene Glycol by Infrared Spectroscopy and X-ray Diffraction Coupled to Differential Calorimetry. Journal of Physical Chemistry B108, 17721-17729.

Chu, Z.Q., Zhang, S.L., Zhang, B.K., Zhang, C., Fang, C.Y., Rehor, I., Cigler, P., Chang, H.C., Lin, G., Liu R., Li, Q., 2014. Unambiguous observation of shape effects on cellular fate of nanoparticles. Scientific Report 4, 4495.

Codoni, D., Belton P., Qi, S., 2015. Nanostructural analysis of water distribution in hydrated multicomponent gels using thermal analysis and NMR relaxometry. Molecular Pharmaceutics 12, 2068-2079.

Date, A.A., Vador, N., Jagtap A., Nagarsenker, M.S., 2011. Lipid nanocarriers (GeluPearl) containing amphiphilic lipid Gelucire 50/13 as a novel stabilizer: Fabrication, characterization and in vivo evaluation. Nanotechnology 22, 275102.

Gref, R., Minamitake, Y., Peracchia, M.T., Trubetskoy, V., Torchilin, V., Langer, R., 1994. Biodegradable long-circulating polymeric nanospheres. Science 263, 1600-1603.

Gustafsson, J., Ljusberg-Wahren, H., Almgren, M., Larsson, K., 1996. Cubic Lipid−Water Phase Dispersed into Submicron Particles. Langmuir 12, 4611-4613.

Gustafsson, J., Ljusberg-Wahren, H., Almgren, M., Larsson, K., 1997. Submicron Particles of Reversed Lipid Phases in Water Stabilized by a Nonionic Amphiphilic Polymer. Langmuir 13, 6964-6971.

Hu, X.L., Hu, J.M., Tian, J., Ge, Z., Zhang, G., Luo, K., Liu, S., 2013. Polyprodrug Amphiphiles: Hierarchical Assemblies for Shape-Regulated Cellular Internalization, Trafficking, and Drug Delivery. Journal of American Chemical Society 135, 17617-17629.

Kelly, S.M., Jess, T.J., Price, N.C., 2005. How to study proteins by circular dichroism. Biochimica et Biophysica Acta Proteins Proteomics 1751, 119-139.

Jollès, P., 1969. Lysozymes: A Chapter of Molecular Biology. Angewandte Chemie International Edition in English 8, 227-239.

Li, X., Chen, D., Le, C., Zhu, C., Gan, Y., Hovgaard, L., Yang, M., 2011. Novel mucus-penetrating liposomes as a potential oral drug delivery system: preparation, in vitro characterization, and enhanced cellular uptake. International Journal of Nanomedicine 6, 3151-3162.

Mitragotri, S., 2009. In drug delivery, shape does matter. Pharmaceutical Research 26, 232-234,

Muro, S., Garnacho, C., Champion, J.A., Leferovich, J., Gajewski, C., Schuchman, E.H., Mitragotri, S., Muzykantov, V.R., 2008. Control of endothelial targeting and intracellular delivery of therapeutic enzymes by modulating the size and shape of ICAM-1-targeted carriers. Molecular Therapy 16, 1450-1458.

Oh, W.K., Kim, S., Yoon, H., Jang, J., 2010. Shape-Dependent Cytotoxicity and Proinflammatory Response of Poly(3,4-ethylenedioxythiophene) Nanomaterials. Small 6, 872-879.

Sharma, G., Valenta, D.T., Altman, Y., Harvey, S., Xie, H., Mitragotri, S., Smith, J.W., 2010. Polymer particle shape independently influences binding and internalization by macrophages. Journal of Controlled Release 147, 408-412.

Shugar, D., 1952. The measurement of lysozyme activity and the ultra-violet inactivation of lysozyme. Biochimica et Biophysica Acta 8, 302-309.

Spicer, P.T., Hayden, K.L., Lynch, M.L., Ofori-Boateng, A., Burns, J.L., 2001. Novel Process for Producing Cubic Liquid Crystalline Nanoparticles (Cubosomes). Langmuir 17, 5748-5756.

Truong, N.P., Whittaker, M.R., Mak, C.W., Davis, T.P., 2015. The importance of nanoparticle shape in cancer drug delivery. Expert Opinion on Drug Delivery 12, 129-142.

Qi, S., Marchaud D., Craig, D.Q.M., 2010. An investigation into the mechanism of dissolution rate enhancement of poorly water-soluble drugs from spray chilled gelucire 50/13 microspheres. Journal of Pharmaceutical Sciences 99, 262-74.

Wang, A.Z., Langer, R., Farokhzad, O.C., 2012. Nanoparticle delivery of cancer drugs. Annual Review of Medicine 63, 185-198.

Zetterberg, M.M., Reijmar, K., Pränting, M., Engström, Å., Andersson, D.I., Edwards, K., 2011. PEG-stabilized lipid disks as carriers for amphiphilic antimicrobial peptides. Journal of Controlled Release 156, 323-328.